Development of Advanced Magnets for Modern and Future Synchrotron Light Sources

Sushil Sharma
NSLS-II/BNL

Acknowledgements

Contributors:

BNL/NSLS-II:
K. Amm, J. Avronsart, A. Banerjee, M. Breitfeller, S. Brooks, O. Chubar, F. DePaola, L. Doom, R. Faussete, R. Gambella, P. Joshi, A. Khan, B. Kosciuk, F. Lincoln, M. Musardo, D. Padrazo, B. Parker, M. Seegitz, T. Shaftan, V. Smalyuk, C. Spataro, T. Tanabe, C. Stelmach, R. Todd, G. Wang

ANL/APSU: C. Doose, A. Jain, M. Jaski
FermiLab: J. DiMarco

For advice and information:

D. Einfeld, P. N'gotta, M. Tischer (PETRA IV)
T. Watanabe (SPring-8), F. Marteau (Soleil), P. Vivian (DLS), P. He (HEPS)
C. Benabderrahmane, G. Le Beck, J. Chavanne (ESRF)
L. Moog, J. Xu (APS)

Outline

1. Introduction
   - Low -emittance storage ring (SR)
     → High strength multipoles of small-bore radii

2. Hybrid permanent magnet (PM) dipoles

3. PM-based quadrupoles – technical challenges

4. Topics from an ongoing R&D Project at NSLS-II :

   Designs of PM-based quadrupoles, field harmonics correction, magnet alignment and magnetic measurements, Vacuum chamber and x-ray beam extraction, Long term radiation damage of PM materials

5. High strength multipoles of conventional (EM) designs

6. Concluding Remarks

Low-Emittance Storage Rings

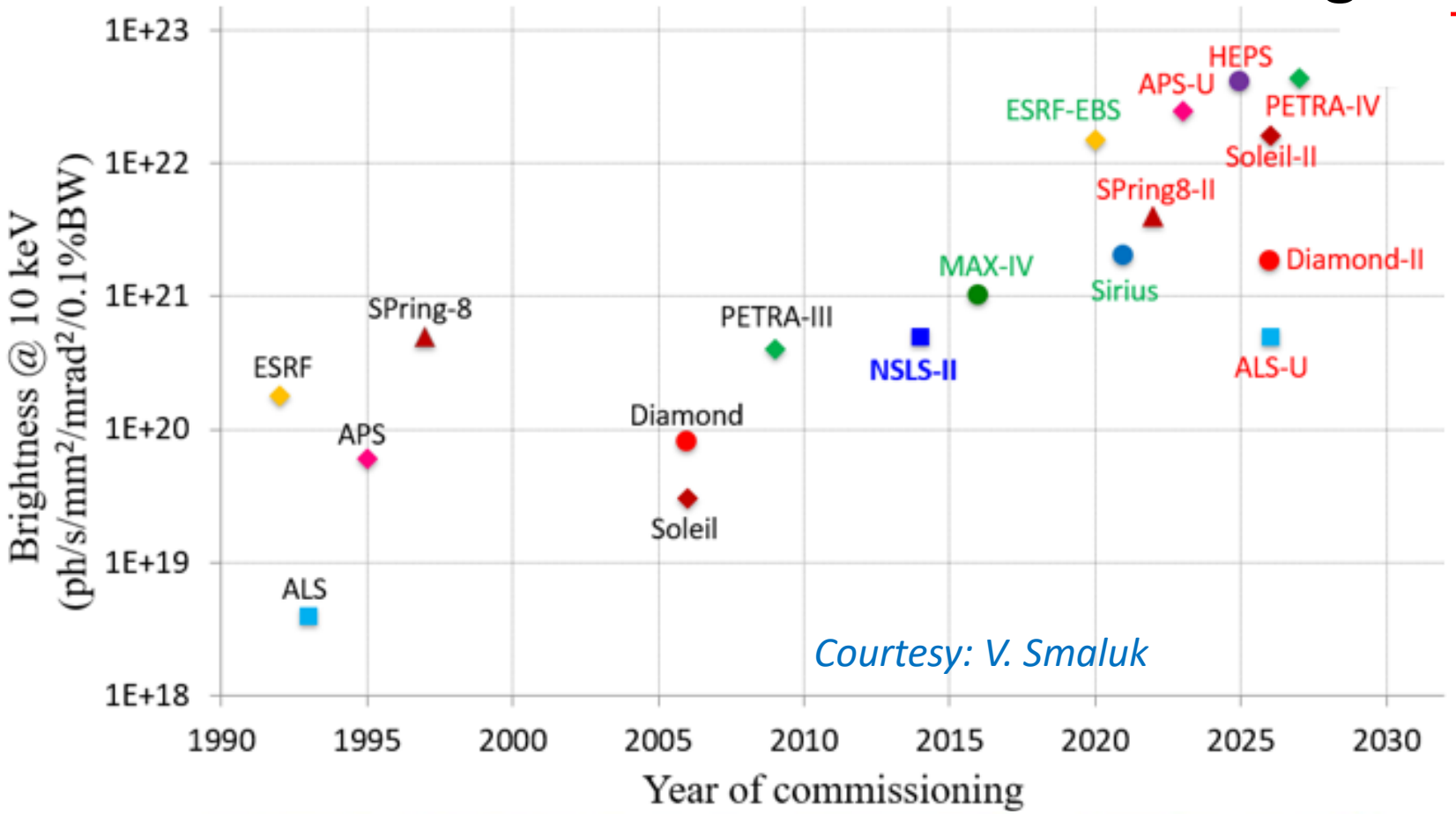

Courtesy: V. Smaluk

APS

NSLS-II

SPS-II

4th generation of storage rings (4GSR) Partial List

Facility	Energy (GeV)	Emittance (pm.rad)
APSU	6	42
ALSU	2	109
DLS-II	3.5	161
HEPS	6	60
NSLS-IIU	3	~ 25
PETRA-IV	6	20*
SLS-II	2.7	160
Soleil-U	2.75	80
SPring-8-II	6	108

**with damping wigglers*

Low-Emittance SR

- Emittance α 1/(nD)^3

  nD: Number of dipoles

  Increase in nD (MBA[1] lattices):

  → moderate strength dipoles

  → high strength multipoles of small-bore radii

  → Large number of magnets of compact sizes

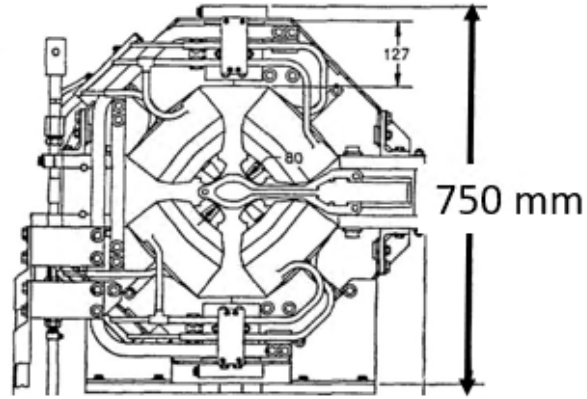

APS (Q4)

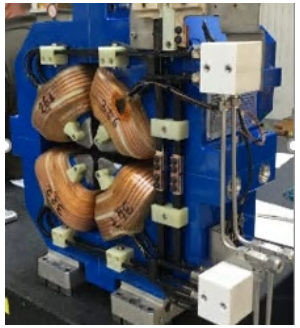

APSU (Q2)

Parameter/Facility	APS (Q4)	APSU (Q2)
Bore radius (mm)	40	13
Gradient, B' (T/m)	19.3	74.3

No. of Magnets

APS	APSU
1100	1355

[1]*D. Einfeld et al., PAC'95, JSR'14*

Low-Emittance SR: NSLS-IIU

- MBA and "Complex Bend[1]" lattices are under evaluation
- In a complex bend high-strength QD and QF quadrupoles are placed in close proximity (~ 30 mm)
- Dipole bending field is generated by combined-function QD and QF, or by an external dipole
- Compact placement of (QD, QF) frees up substantial space in the lattice while enabling a path towards ultra low emittance
- A possibility to integrate super-bends into CB for BM beamlines
- Small spacing between (QD, QF) → No coils, only PM-based quads, but EM multipoles, Q,S,O, outside CB
- High strength QD, QF → bore radius is ~ 8 mm

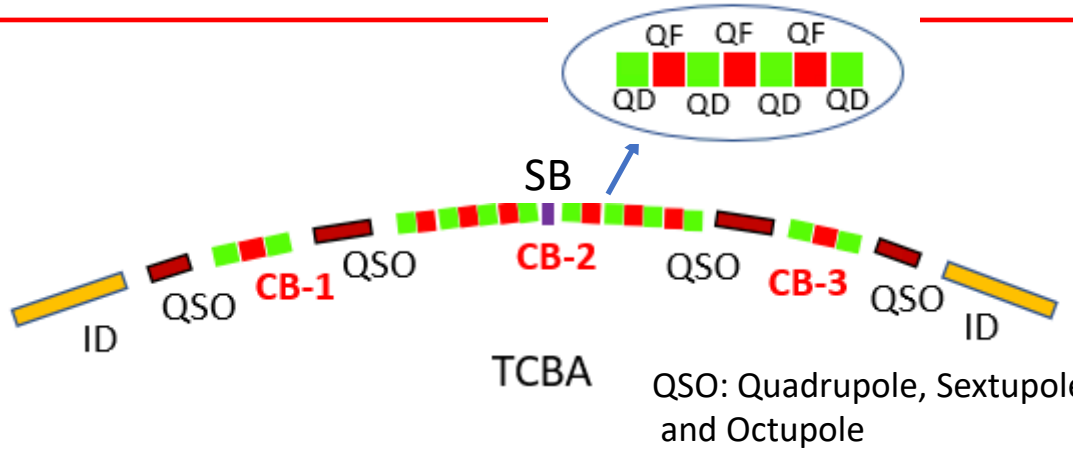

NSLS-II EM Quad

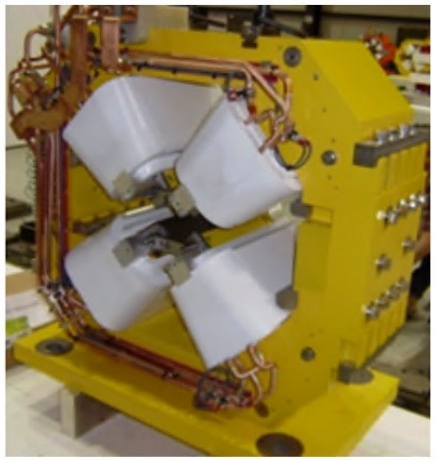

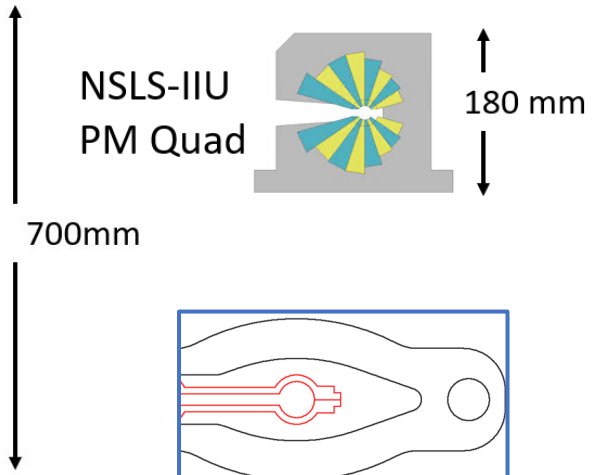

Vacuum Chamber Apertures
NSLS-II / NSLS-IIU

Quadrupole	NSLS-II	NSLS-IIU
Bore radius (mm)	33	~8
Gradient, B' (T/m)	20.0	~130

[1] *T. Shaftan et al. NSLSII Tech. Note [2018]*

Hybrid PM Dipoles

Facility	APSU[1]	ALSU[1]	DLS-II	ESRF-EBS	HEPS	PETRA - IV[2]	Soleil-U	SPring-8-U
Field (T)	0.153-0.729	1.069	0.29 – 0.76	0.17 – 0.67	0.11 – 1.0	0.223 – 0.287	0.7 T	0.193 – 0.791
Transverse Grad. (T/m)		20.01				9.09 – 11.69	16.0	
Pole Gap (mm)	27	NA	25	25.5	27	NA	NA	25

APSU M1

EM Dipole

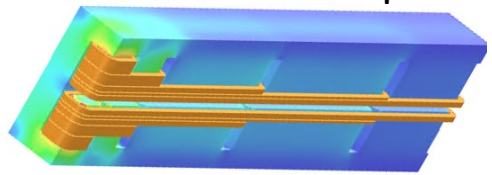

[1]EM Designs, [2]both Longitudinal and Transverse Gradients (LG and TG)

- Transverse gradient is included in the dipoles of ALSU, Soleil-U and PETRA IV
- Strong trend towards hybrid PM dipoles
  - No operational cost
  - No utilities (power supply, water)
  - No vibration
  - Dipoles are compact in size

ESRF-EBS Dipole

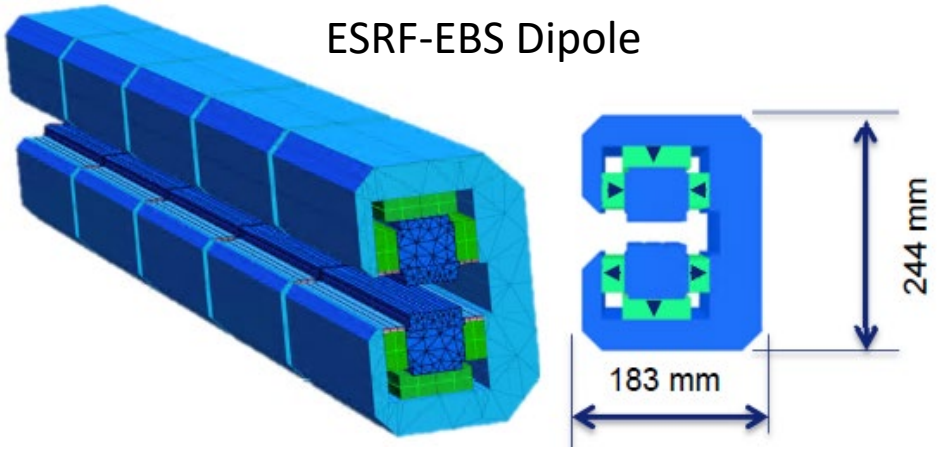

C. Benabderrahmane et al., IPAC2017

Hybrid PM Dipole

PETRA IV

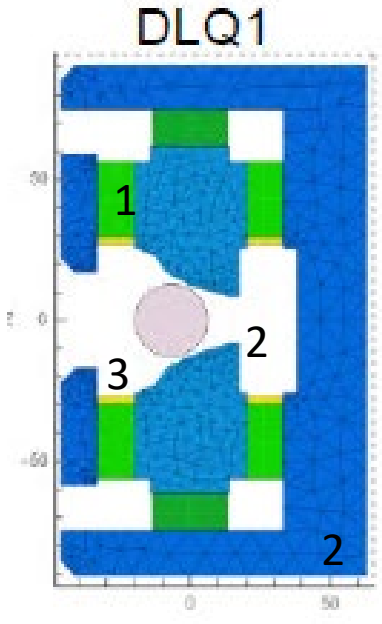

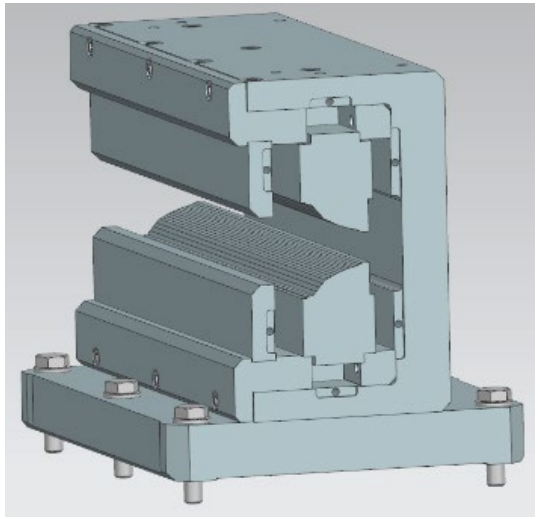

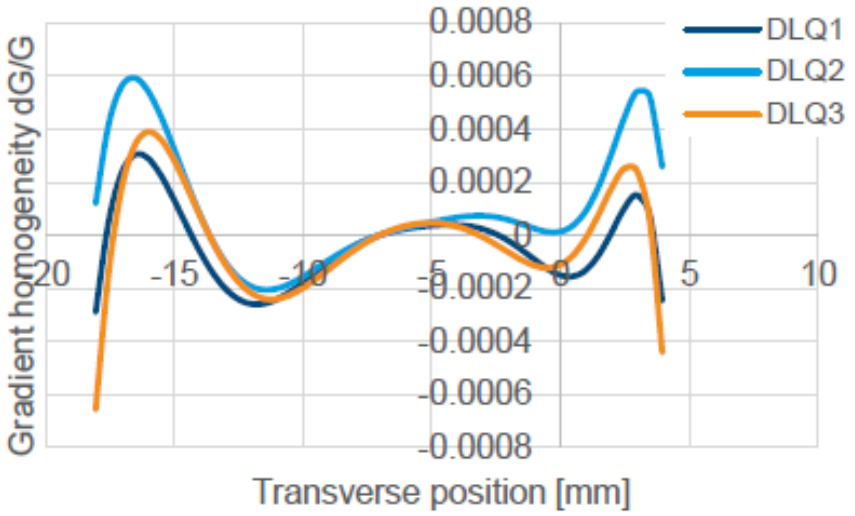

DLQ1 Field Strength[1]

Dipole (T)	0.223 – 0.287
Gradient (T/m)	9.09 – 11.69

4 segments,
0.303 m long

[1]*D. Einfeld, Private Comm. May 2022.*

1 →PM Magnets: SmCo (green)
2 →Poles and Backleg: Armco steel (blue)
3 → Thermal shims: FeNi (yellow)

M. Tischer / J. Chavanne, PETRA IV TAC Meeting, March 2022

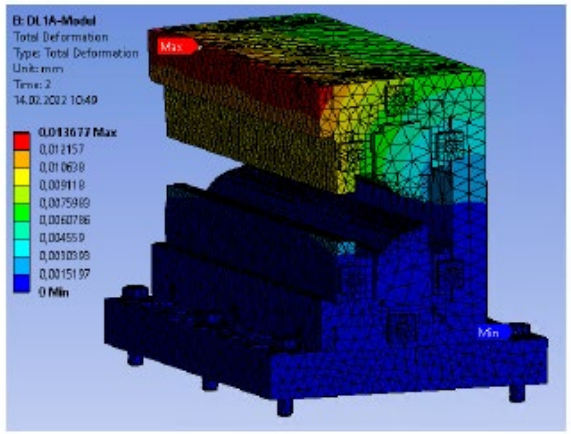

Court. T.Ramm

Hybrid –PM Dipole (Contd.)

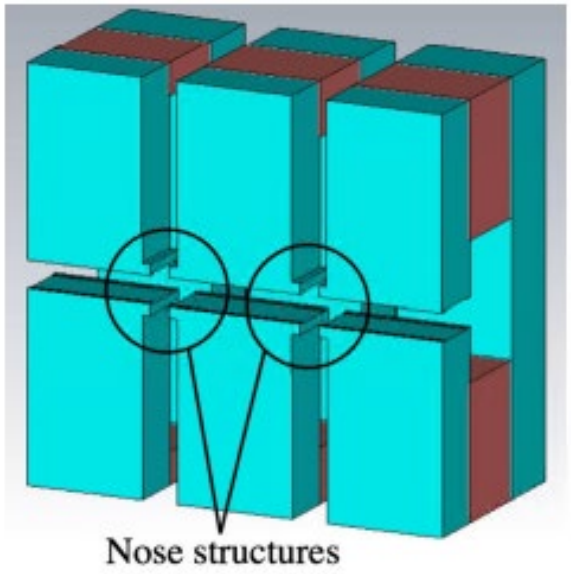

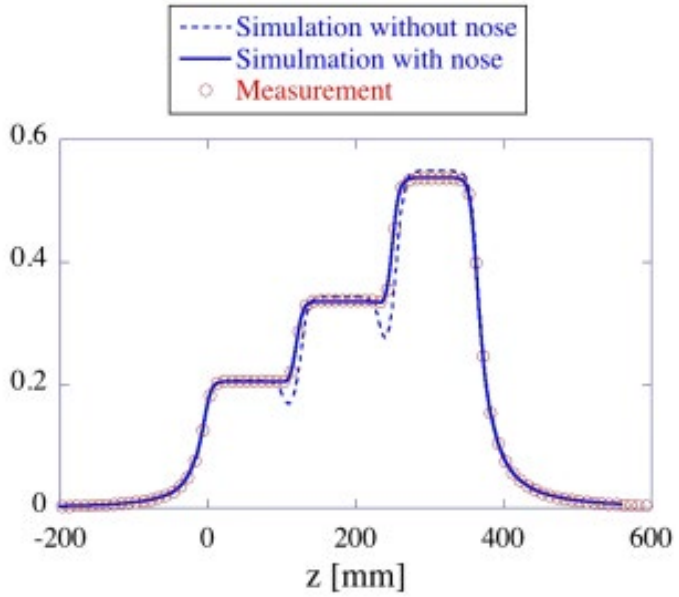

[1]Test LG Dipole for SPring-8-II

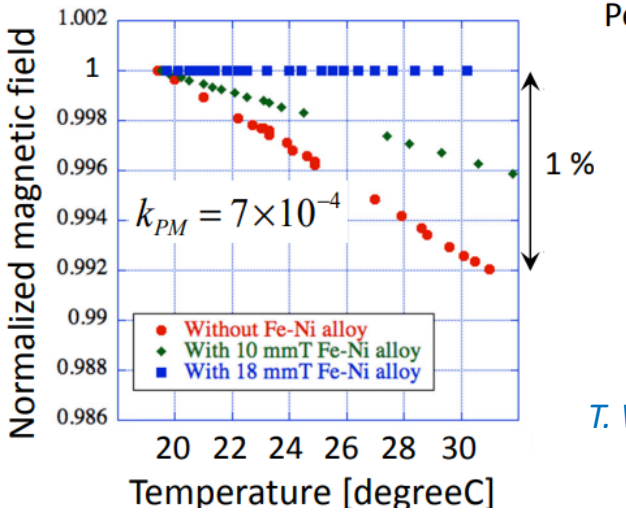

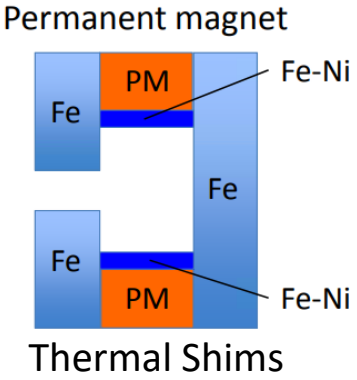

T. Watanabe et al., IPAC'16

B_r of PM materials is temperature dependent. Temperature stability can be improved by FeNi shims.

- LG hybrid-PM dipoles are being developed for SPring-8-II.
- Dipole field adjustments by nose structures, FeNi thermal shims, and movable outer plates have been investigated.

[1]*T. Watanabe et al. PRAB 20 (2017)*

Dipole of Adjustable Field with Outer Plates

Dipole Options for NSLS-IIU Complex Bend

- Combined-function high-gradient PMQs for NSLS-IIU are expected to require large harmonics corrections.
- Another option is to place symmetric Halbach PMQs inside a varying field “saw tooth” dipole. Unlike LG dipoles(EM), this dipole uses a single coil.
- A complex bend prototype dipole with pole gaps of 90 mm, 128.4 mm and 180 mm is being investigated by Opera models.
- Magnetic design of a hybrid-PM version with a constant gap of 90 mm is also in progress.

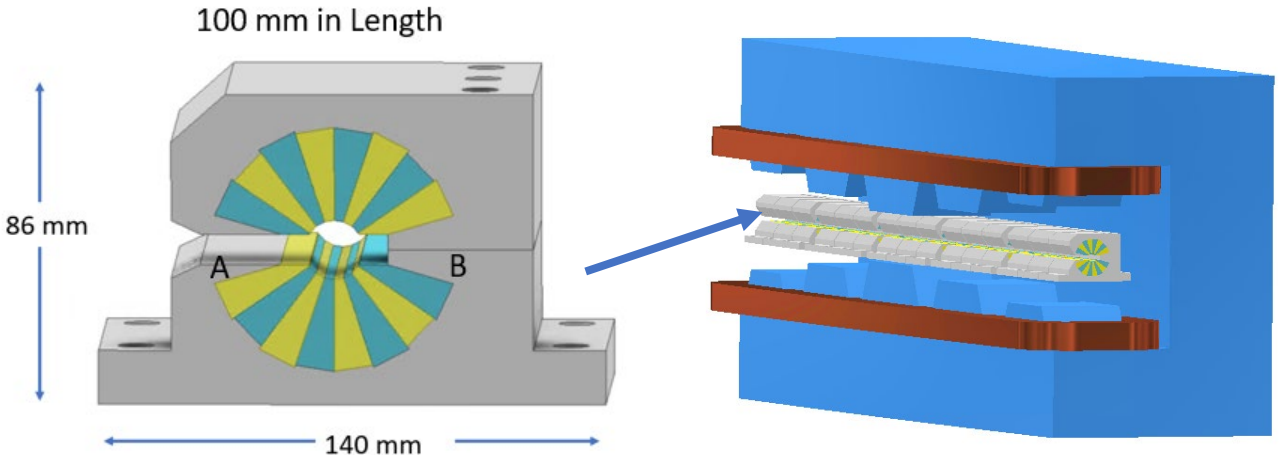

Symmetric Halbach PMQ

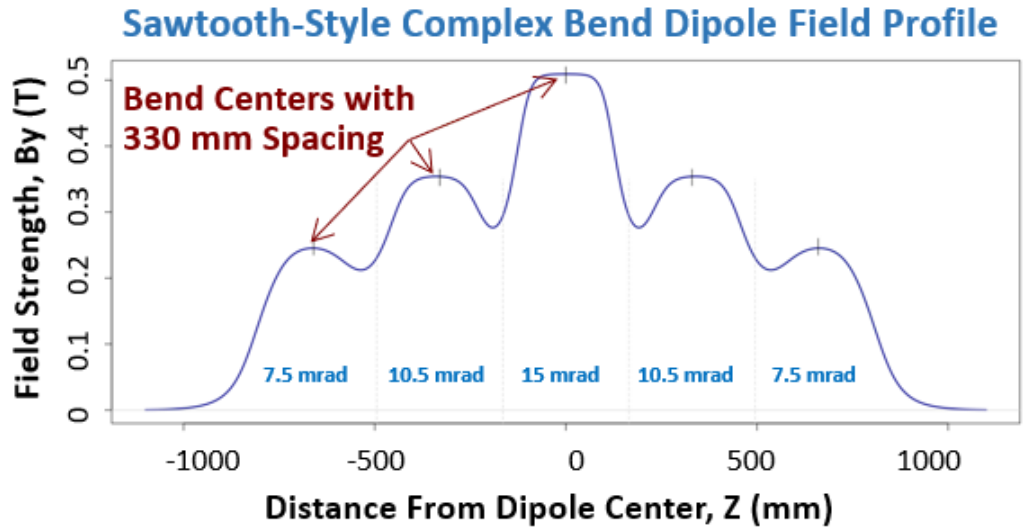

Technical Challenges with PM-Based Quadrupoles

- Tunability
  - ➢ No practical and reliable solution → EM Family of adjacent quadrupoles and corrector coils
- Thermal stability of the magnetic field → FeNi shims; SR tunnel with ± 0.1^{o}C temperature control
- Field Harmonics errors due to fabrication tolerances
  - ➢ Magnetic properties of PM wedges/blocks (B_r , Θ_m)
  - ➢ Machining and assembly errors
- Magnet alignment and magnetic measurements of small-bore magnets with high field gradients
- Small aperture (~ 10mm) vacuum chamber and x-ray beam extraction through a narrow exit slot (~ 3 mm)
- Long-term radiation damage of PM materials

PM-based Quadrupoles – Halbach Style

- Halbach-style magnets consist purely of PM wedges (no iron). The sizes and magnetization angles (θ_M) of the PM wedges determine the multipole field.
- Halbach symmetric and combined-function (CF) PMQs have been built for CBETA ERL.
- High gradient symmetric Halbach PMQs are compact in size especially for small bore radius (~10 mm)
- For light sources, an exit slot is required for the vacuum chamber and x-ray beam extraction. An open mid-plane design meets this requirement[3]. The sizes and magnetization angles are optimized for the open mid-plane.
- Large field errors because of tolerances in the wedge dimensions, θ_M and assembly.

Halbach PMQ[1]

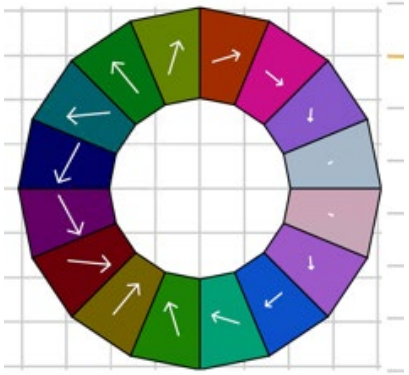

CBETA C-F PMQ[2]

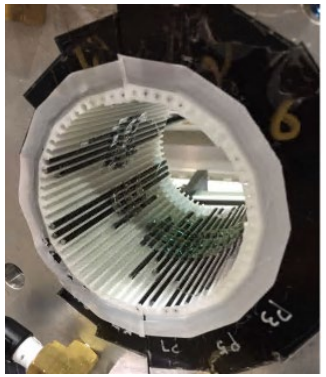

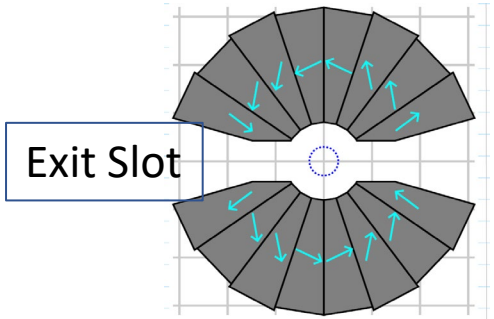

Symmetric PMQ

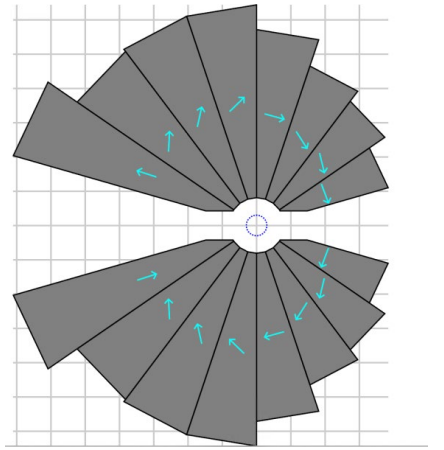

Combined-Function PMQ

[1]*K. Halbach, NIM (1980)*, [2]*S. Brooks et al., PRAB (2020),* [3]*N. Tsoupas et al. NAPAC (2016)*

Magnetic Design – Symmetric PMQ for NSLS-IIU

PM Material: RS32HS
https://www.shinetsu-rare-earth-magnet.jp/e/products/data_sm.html
Br = 1.167 T, Hc = 873,670 A/m, μ_r = 1.063, Linear and Isotropic

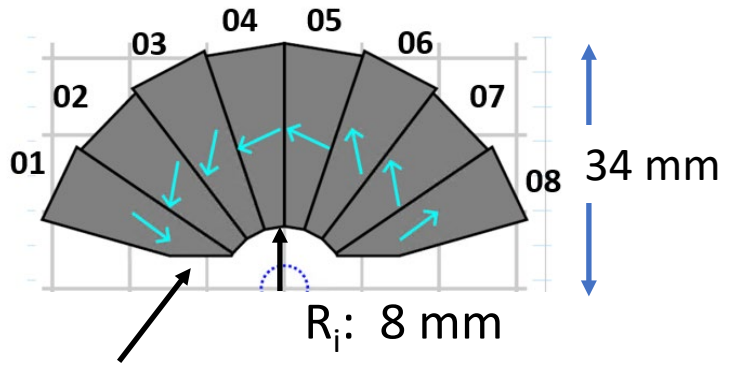

Exit slot: 8.5 mm

Magnetization Angles θ_M from X-axis:

Wedge	1	2	3	4	5	6	7	8
Angle θ_M (Deg)	-36.05	-99.76	-101.04	-154.31	154.31	101.04	99.76	36.05

Wedges (9-16) are obtained by mirror symmetry and adding 180^o to θ_M.

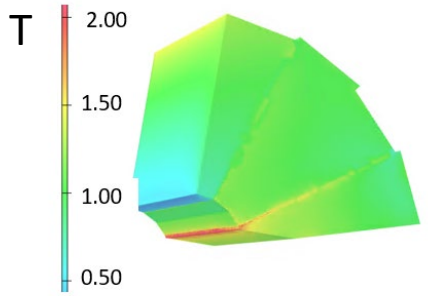

Surface Magnetic Flux (B)

Q Gradient (B') = 130 T/m

Normalized Harmonics of symmetric PMQ at R_{ref} = 3 mm

B_n	1	2	3	4	5	6	7	8	9	10
Value x e04	1.0 e04	0.0	0.1	0.0	0.9	0.0	4.1	0.0	0.3	0.0

RSS (root-sum-square) error of $B_2 - B_{10}$ = 4.2 e-04 < 5.0 e-04 (specification)

Magnetic Design: Combined-Function PMQ for NSLS-IIU

Magnetization angles θ_M from X-axis

Wedge	1	2	3	4	5	6	7	8
Angle θ_M (Deg)	252.20	257.36	239.79	195.61	135.84	103.57	92.56	17.43

Wedges (9-16) are obtained by mirror symmetry and adding 180^o to θ_M

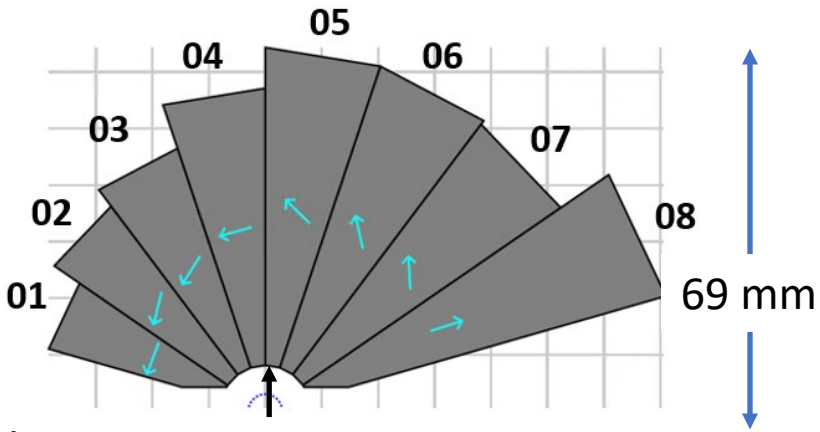

Exit slot: 8.5 mm R_i: 8 mm

Normalized Harmonics of combined -function PMQ at R_{ref} = 3 mm

B_n	1	2	3	4	5	6	7	8	9	10
*Value x e04	1e04	0.0	1.5	0.1	0.9	2.8	5.6	3.1	0.1	0.1

*Preliminary Optimization

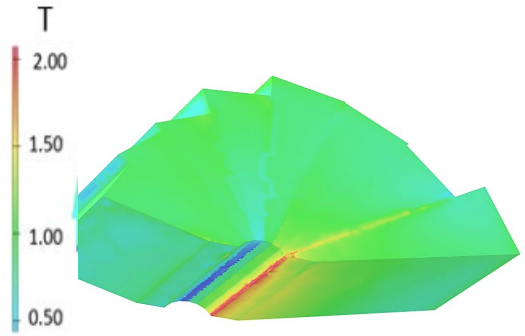

RSS error of $B_2 - B_{10}$ = 7.0 e-04 > 5.0 e-04 (specification)

- The size increases by ~60% compared to the symmetric version
- A 16-wedge design, with R_i = 8 mm, and exit slot of 8.5 mm can provide 0.5 T dipole field and 130 T/m quadrupole gradient.

Dipole Field = 0.5 T
Q Gradient = 130 T/m

Mechanical Design- Symmetric PMQ

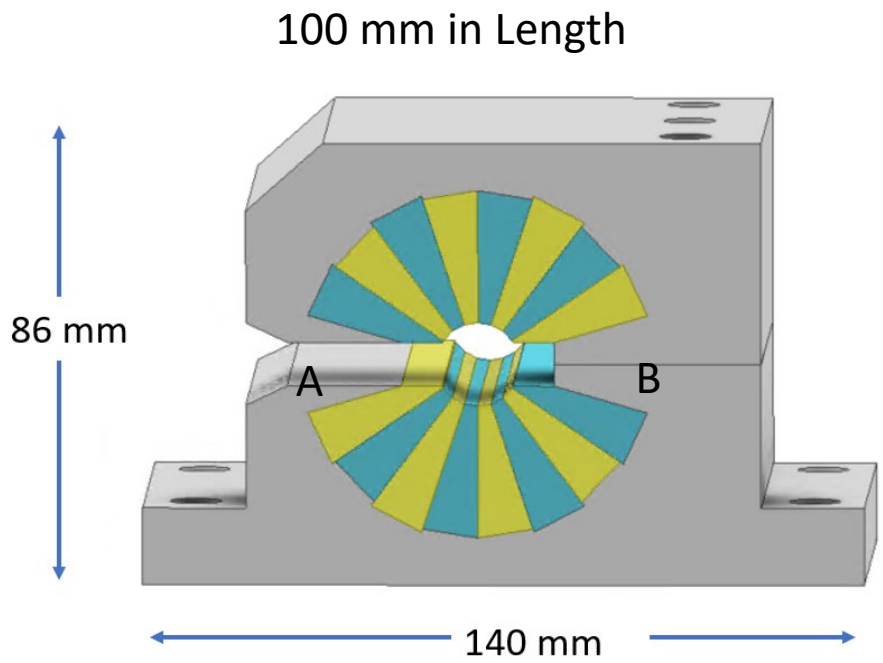

- The aluminum housing is split in the mid-plane to install the vacuum chamber.
- Two pairs of tabs (A and B) in the housing provide restraining support to the PM wedges against magnetic forces.

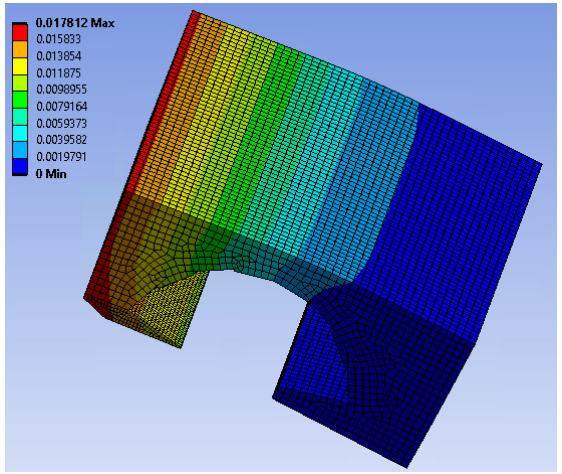

Magnetic Force on Clamshell = 729.1 N
Max. Deflection: 17.8 µm

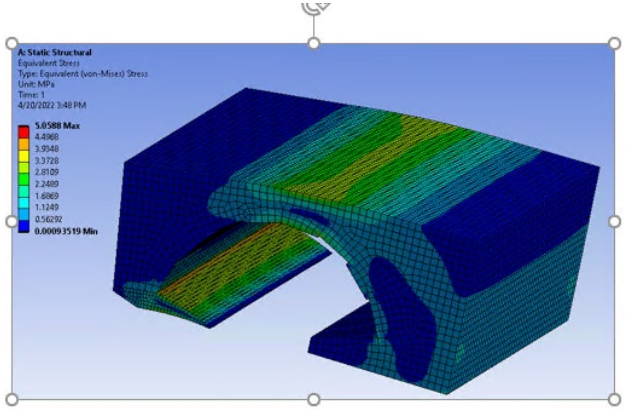

Magnetic Force on the upper tab A = 349.7 N
Max. Stress = 5.1 MPa

Hybrid PM Quadrupole for NSLS-IIU

- Based on PETRA IV design.
- Less sensitive to θ_M, and machining/assembly tolerances
- Bore radius of 11 mm:
  - ➢ Gradient: 140 T/m
  - ➢ 3 mm offset → ~ 0.42 T dipole field.
- Field error $\Delta G/G_0$ < 7.1 e-04 in the GFR (± 3 mm)
- Pole shaping and "magic fingers" can be used to reduce higher harmonics.
- *Higher leakage field compared to Halbach PMQ.*

M. Tischer /J. Chavanne
PETRA IV TAC Meeting, March 2022

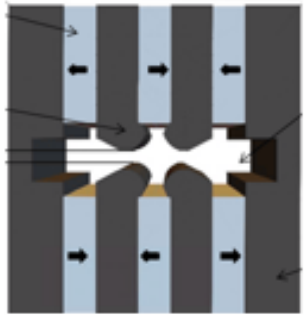

Hybrid PMQ
P. N'gotta et al, PRAB [2016]

PETRA IV

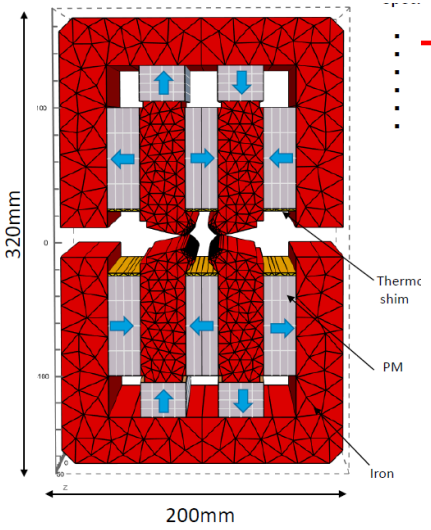

Vanadium-Permendur

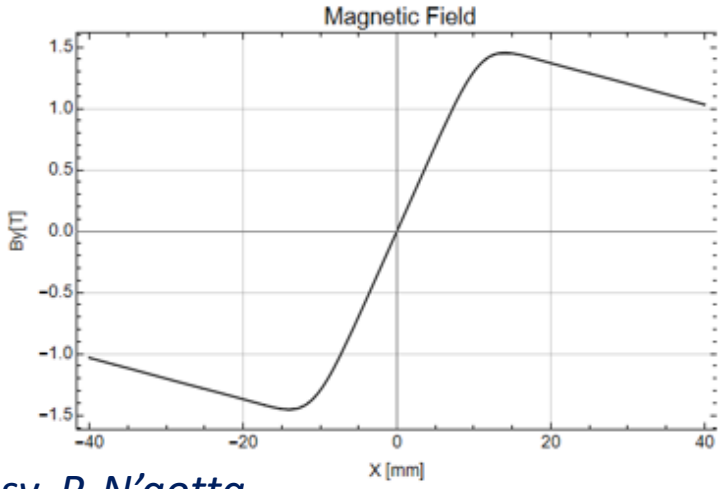

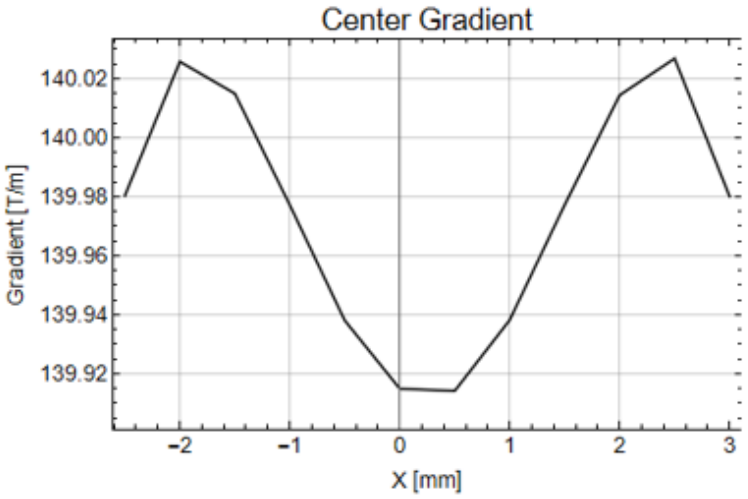

Courtesy, P. N'gotta
May 2022

Field Harmonics Errors in PMQs

- Large field harmonics errors due to tolerances of B_r, θ_M and R_i. Machining and assembly tolerances are combined in R_i.
- The RSS (root-sum-square) of these errors for Halbach PMQ is ~ 175 e-04 for random changes within maximum tolerances
- The field error is dominated by the tolerance of θ_M and is characterized by large dipole (b_0) and skew quadrupole (a_1) components
- In a hybrid PMQ the field error is dictated by machining and assembly errors of the iron poles. These can be controlled to ~ 20 μm and the resulting harmonics errors to ~1 e-03

NSLS-IIU Prototype PMQ of 100-mm length

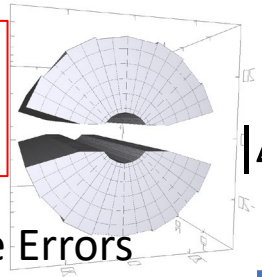

With Magnetic & Geom. Errors
$|\Delta B_r/B_r| < 0.015$, $|\Delta\theta_M| < 1.5°$
$\Delta R_i < 100$ μm

No tolerance Errors

No.	A_n x e04	B_n x e04
0	0	0
1	0	1,0 e04
2	0	0
3	0	0.0032
4	0	0
5	0	-0.405
6	0	0
7	0	-4.122
8	0	0

No.	A_n x e04	B_n x e04
0	28.3	124.24
1	-119.1	1.0 eo4
2	-10.64	-3.672
3	8.383	-2.18
4	-0.036	-2.535
5	0.153	0.526
6	-0.069	0.168
7	-0.063	-3.923
8	0.035	0.018

RSS = 175 e-04

Harmonics Correction by Alignment and "Magic Fingers[1]"

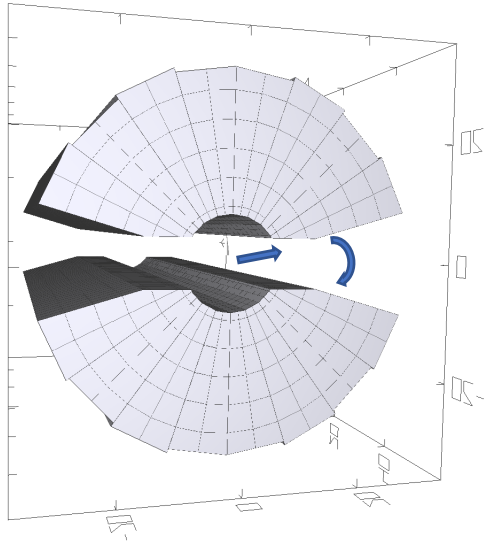

After PMQ Shift by $\Delta x_c \approx 37$ μm, $\Delta y_c \approx 9$ μm and Rotation by $\Delta\varphi \approx -5.9$ mrad

Field Harmonics

No.	A_n x e04	B_n x e04
0	-0.025	-0.024
1	-0.11	1.0 e04
2	-10.989	-3.322
3	8.364	-2.255
4	-0.129	-2.562
5	0.165	0.495
6	0.039	0.505
7	-0.253	-3.917
8	0.045	0.045

RSS = 15.1 4e-04

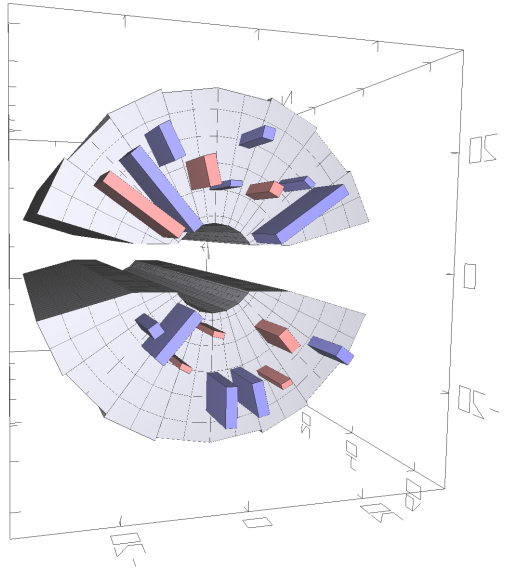

MF PM blocks (2mm x 2 mm x ~8mm) are stacked radially as needed. The colors of the PM blocks represent their different magnetization directions.

Field Harmonics

No.	A_n x e04	B_n x e04
0	0.17	0.37
1	-0.52	1.0 eo4
2	-0.066	-0.167
3	0.762	0.971
4	-0.062	-2.348
5	0.235	0.013
6	-0.236	0.459
7	-0.179	-3.918
8	0.051	0.036

RSS = 4.8 e-04

[1] *E. Hoyer et al, RSI 1995*

Rotating-Wire System for Magnet Alignment

- The NSLS-II R-W system is based on the hardware design and software developed for APSU
- The primary use is to establish magnetic center and relate it to magnet fiducials for subsequent alignment in a module
- Based on R&D at APSU, the magnetic center can be reproduced using the fiducials with an RMS error of < 5 μm
- The rotary stage at each end is mounted on XYZ linear stages which permit the wire loop to be stretched and positioned transversely within the magnet aperture
- The voltage induced by the rotating wire is digitized and processed to obtain the magnetic center offset and field harmonics
- Laser Trackers are used to record the magnet and bench fiducials after the wire rotation axis is placed at the magnetic center

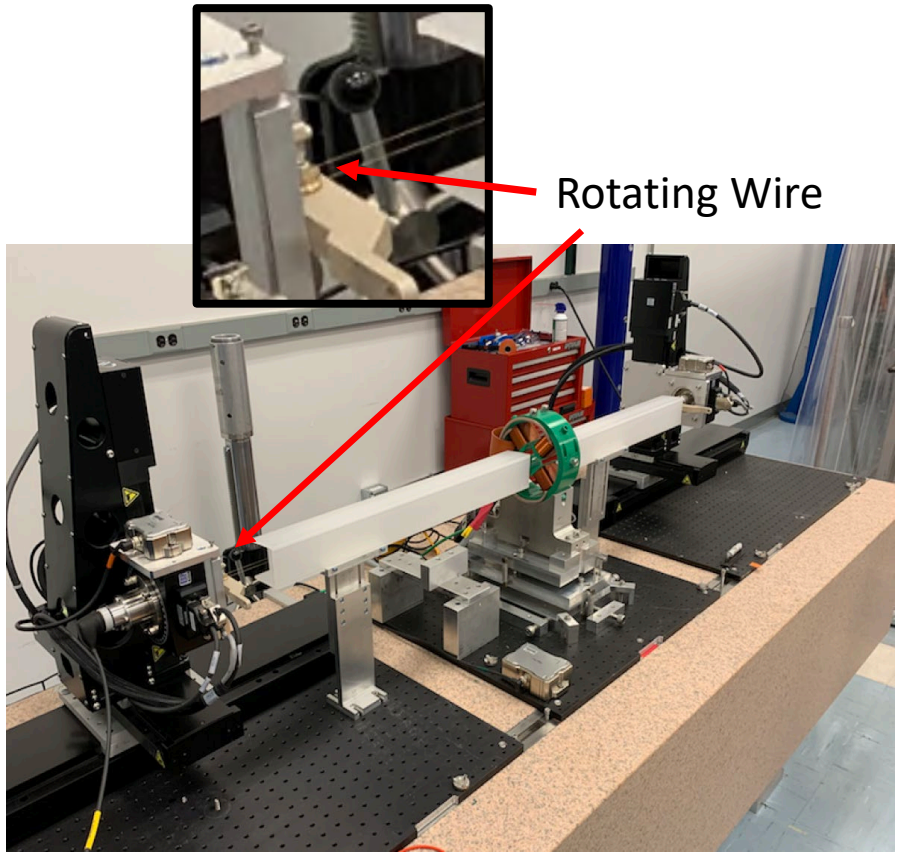

Rotating-Coil Magnetic Measurement System

- A 12-mm diameter PCB-based rotating coil was designed at FermiLab with specifications of 10 ppm of the main field (0.1 “unit”) up to the 15th harmonic at the reference radius of 5 mm. Three PCB coils were built.
- The PCB coil is encased in carbon fiber supports to ensure sufficient stiffness against vibration and sag.
- The R-C system uses essentially the same hardware and software for motion control as the R-W system.
- For high signal amplitude, the PCB coil is designed with a high density of turns (75 µm wide traces with 75 µm apart) in 16 layers.
- The PCB coil has the capability of providing un-bucked (UB), dipole bucked (DB), dipole-quad bucked (DQB) and dipole-quad-sextupole bucked (DQSB) signals, in order to ensure minimal spurious harmonics in measurements of both quadrupole and sextupole magnets.

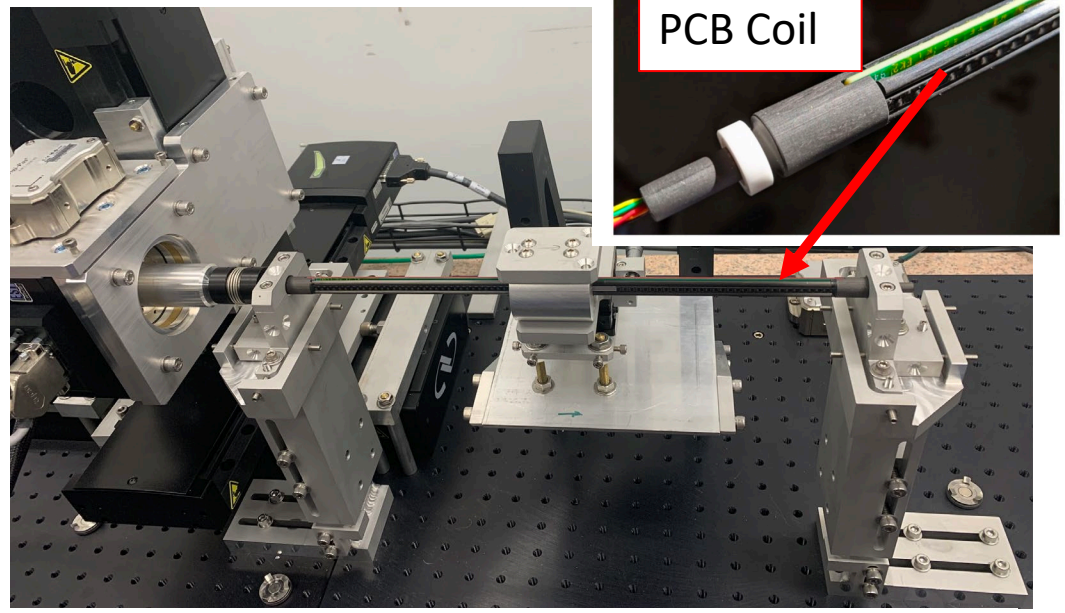

Probe Diameter	12mm
Reference Radius	5mm
Resolution	0.1 unit
Probe Active Length	250mm
Length of each end stem	25mm
Total Probe Length	~350 mm
Bucking	DB, DQB, DQSB

Dipole Magnetic Measurement Bench Upgrade

Senis 3MH6
Digital Tesla Meter

Metrolab Digital
NMR Teslameter

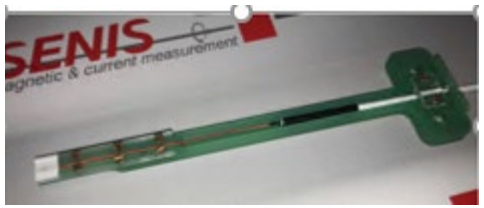

Probe Holder

Type	Model
Metrolab Digital NMR Teslameter	PT2026
NMR PW probe Wide Range 0.2-3T	1326-0.20-0.30
Senis 3 axis Digital Teslameter	3MH6
Probe holder for C-type transducers	PHS-DL

- Probe and probe holder height < 3.6 mm (slot height)
- New hall probe with 0.01% accuracy
- Bench accuracy is being measured → upgrade to 1 µm
- Temperature stability → upgrade to ± 0.1°C

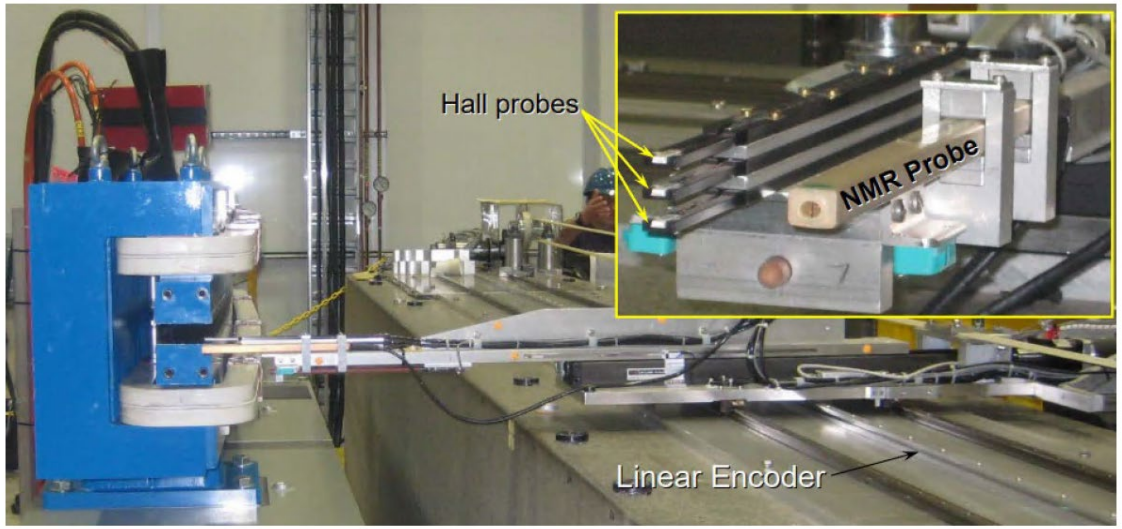

Prototype Small-Aperture Vacuum chamber

- The chamber is to be fabricated from machined aluminum halves.
- Resistive wall heating is acceptably low, 13 W/m.
- Power loss from geometric impedance is negligible (<1 W/m) with and resonance peaks occur at > 15 GHZ

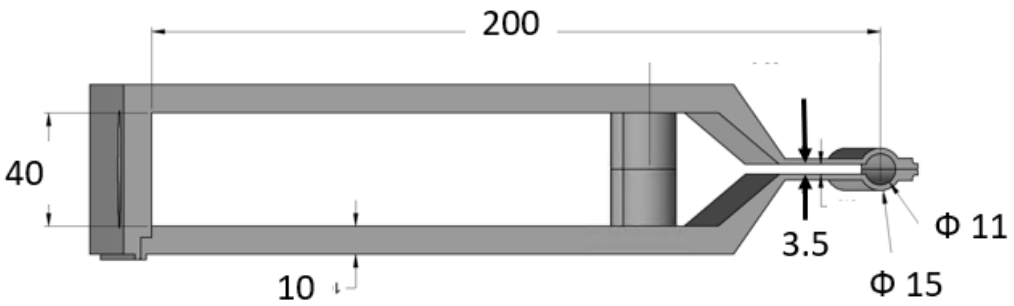

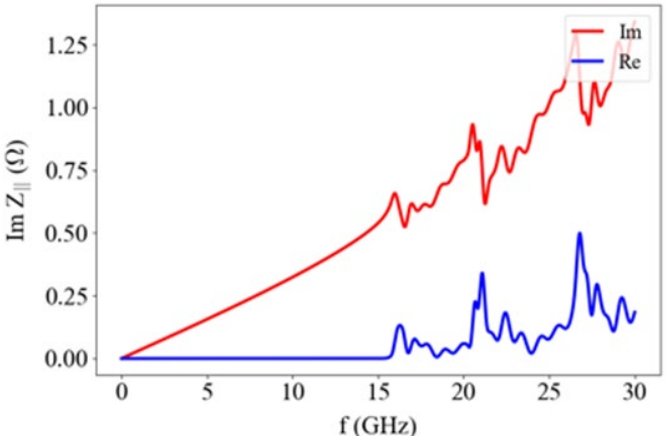

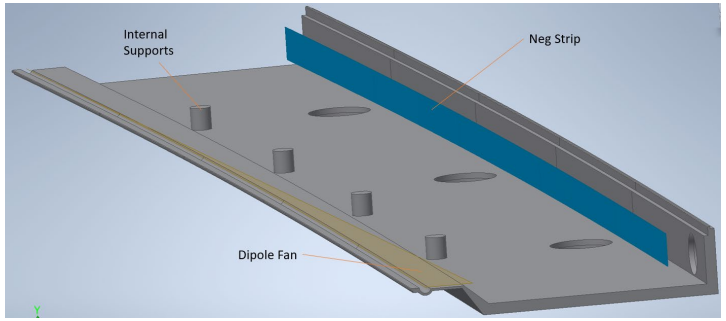

Chamber-half with internal support

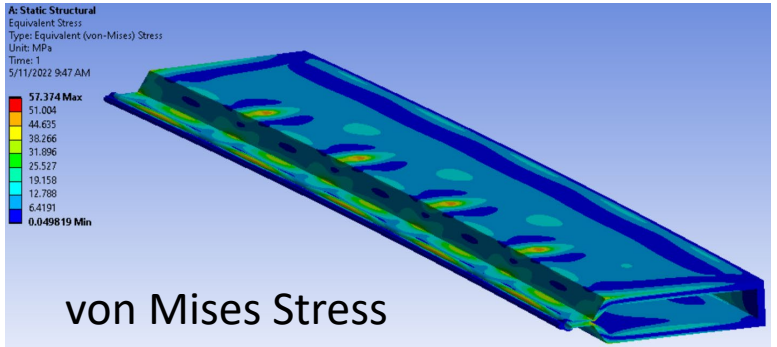

von Mises Stress

- Maximum stress and deflection, 57 MPa, 0.2 mm, are held within allowable levels with internal supports.
- MolFlow calculations show adequate vacuum (< 7 e-09 mbar) with three 150 l/s ion pumps. Neg strips can provide additional pumping
- 3.5mm exit slot conductance sufficient to provide adequate pumping to the beam channel.

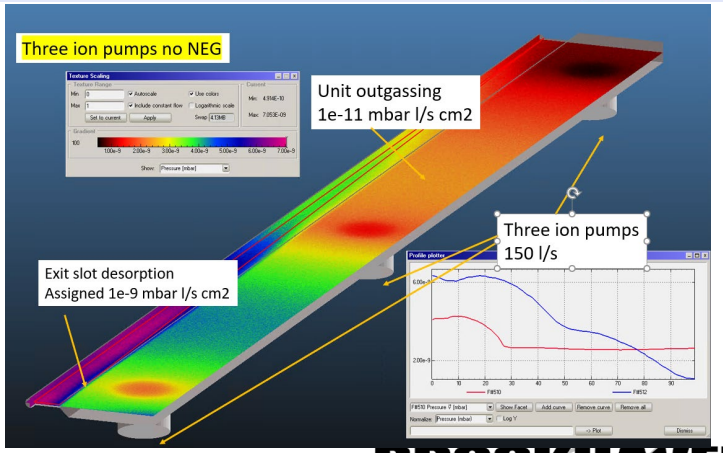

X-ray Beam Extraction

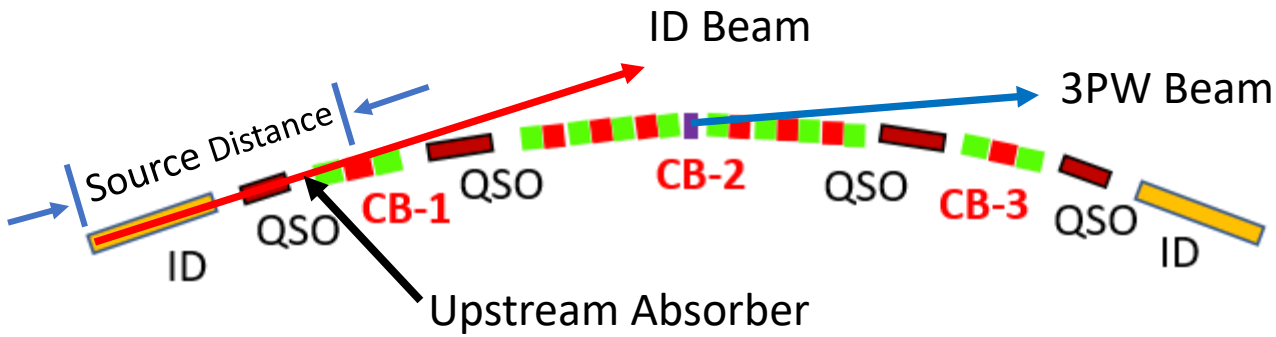

3PW Beam:

Source Distance = 2.50 m

Beam Height = 2.50 m * 1.2 mrad = 3.0 mm ✓

ID Beam:

Source Distance: ~ 12 m

Beam Height = 10 m * 1.2 mrad = 12 mm ✗

→ Increase vacuum chamber slot to 6 mm and trim the ID beam by an upstream absorber

→ Magnet pole-tip gap: 11 mm

→ Maximum strength of the 1st PMQ: ~ 105 T/m

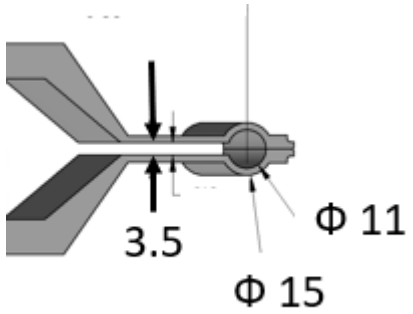

Total Power = 8.11 kW

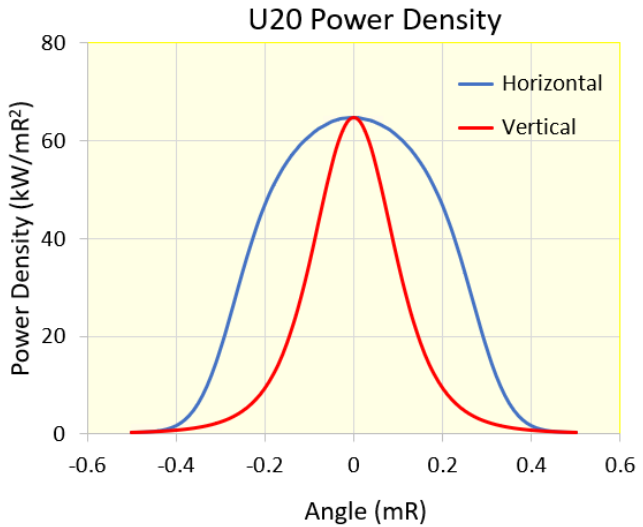

Beam Deviation Interlock: ± 0.1 mrad

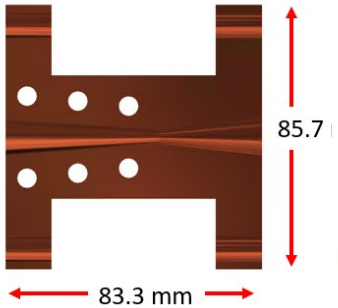

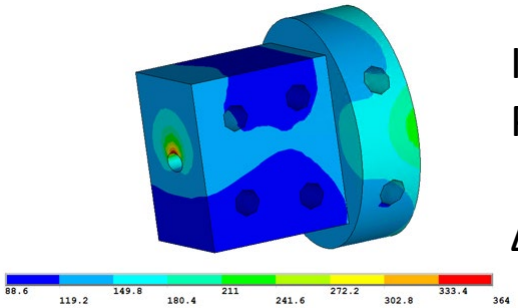

Intercepted Power : 2.5 kW

ΔT = 364°C

Upstream absorber with tapered aperture

Long-Term Radiation Damage of PM Materials

- Sm_2Co_{17} has higher radiation hardness than $Nd_{2-x}Fe_{14}B$ [1,2].
- Demagnetization characteristics depends not only on Hcj but also the operating point (permeance) of the magnetic circuit.→ single block test is not sufficient [3].
- Long term radiation damage will be measured by precisely measuring changes in the harmonics of PMQs after long-term exposures in the Linac test beamline and C20 front end.
  - 15 Halbach style PMQs from CB prototype
  - Bore Radius = 8.0 mm, Length = 100 mm
  - Gradient = 130 T/m
  - PM Material: Sm_2Co_{17}

Halbach PMQs

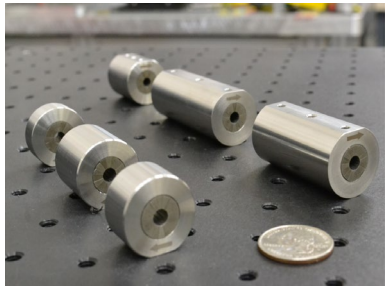

Linac Test Beamline

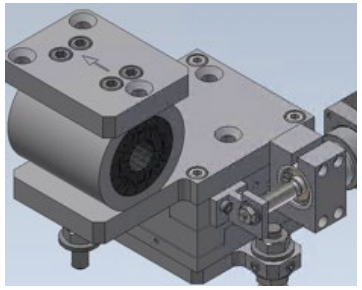

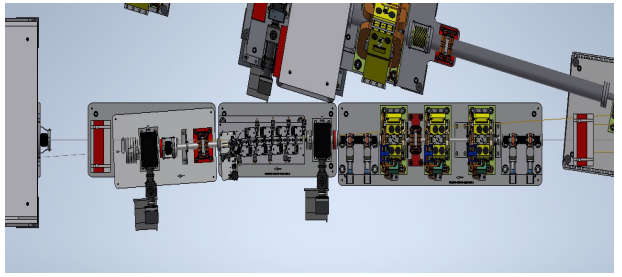

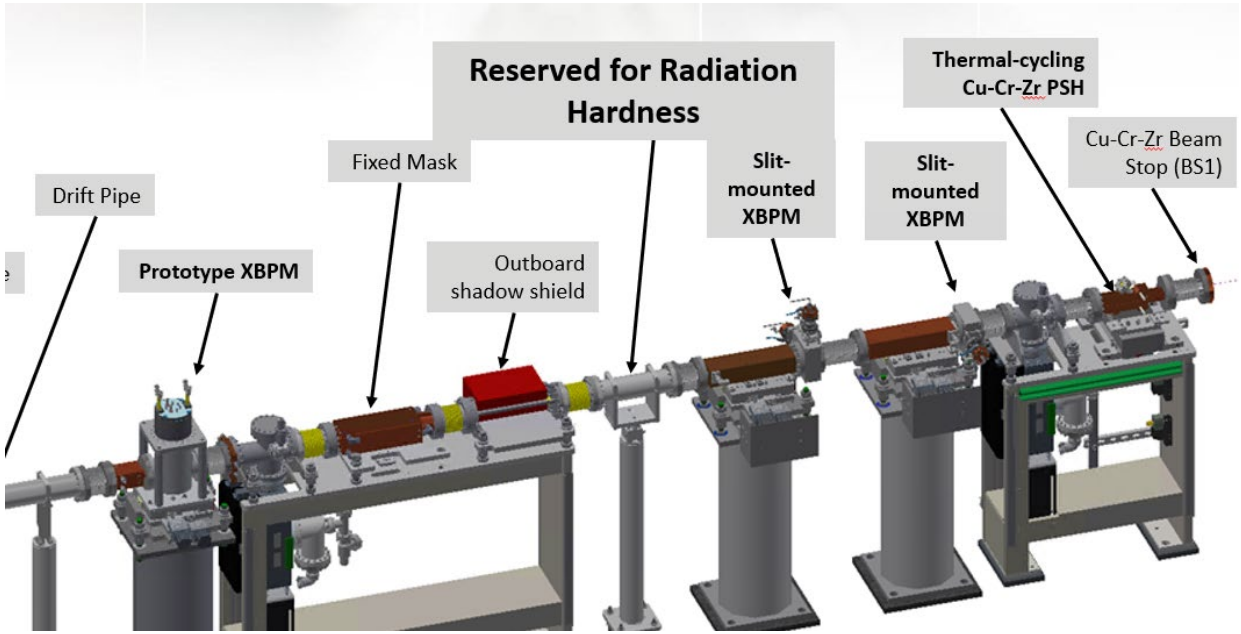

C20 Front End

[1] R.D. Brown et al., 1985, [2] O-P Kahkonen, et al. 1990, [3] M. Baltay et al. PAC'87

High Strength EM Quadrupoles

Facility	APSU	ALSU	DLS-II	ESRF-EBS	HEPS	PETRA-IV	Soleil-U	SPring-8-II
B' (T/m)	94.9	109	90	89	90	115.2	120	56
Bore R (mm)	13	12	12	12.6	13	11	8	17

APSU (Q7)

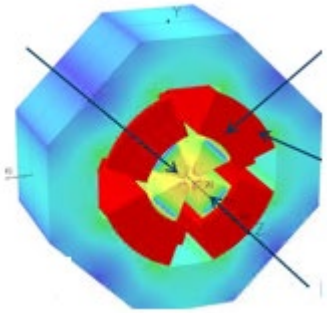

ALSU (QFRD)

- Small bore radius
- Solid yoke of soft iron (1010)
- High permeability FeCo (Vanadium Permendur, Vacoflux) pole tips
- Pole-shaping and end chamfering for good field uniformity ($\Delta G/G_0 \leq 10^{-3}$)
- Poles are usually saturated. Efficiency 90% (APSU) to 98% (ALSU)

VP Pole Tip

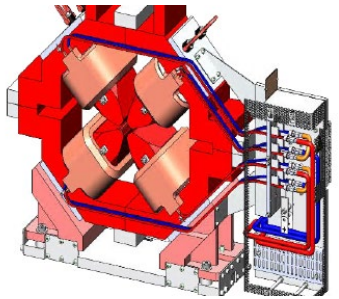

ESRF-EBS

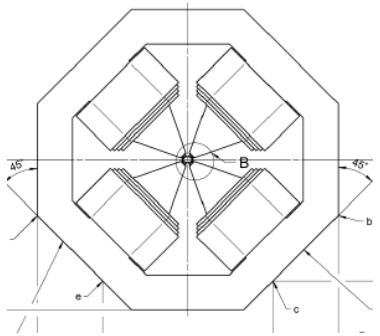

PETRA IV

High Strength EM Quadrupole (contd.)

APSU Q7

Parameter	Value
Bore Radius	13 mm
Pole-tip gap	10.2 mm
Q-Gradient	97.3 T/m
Current	7284 ampere-turns

Bore radius/Pole-tip gap ≥ 1.3 for good field harmonics.

NSLS-IIU Quadrupole:
Bore radius = 8 mm
Pole-tip gap = 8 mm
Gradient = 132.2 T/m at 99% efficiency
= 173.8 T/m at 90% efficiency

- At R_{ref} = 3 mm, B_3 = 0.03 e-04, B_5 = 1.4 e-04

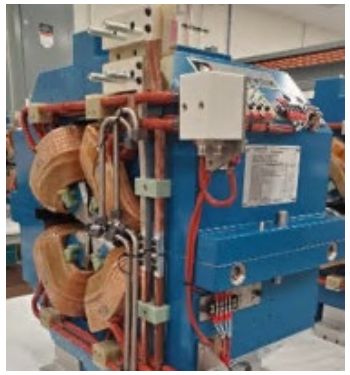

APSU Q7

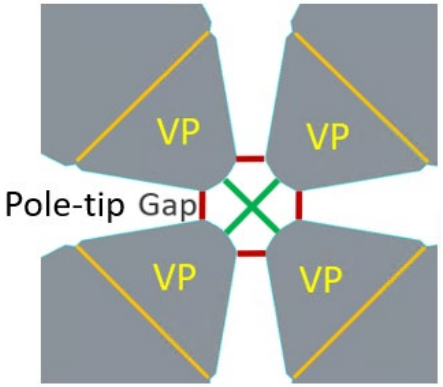

Vanadium-Permendur Pole Tips

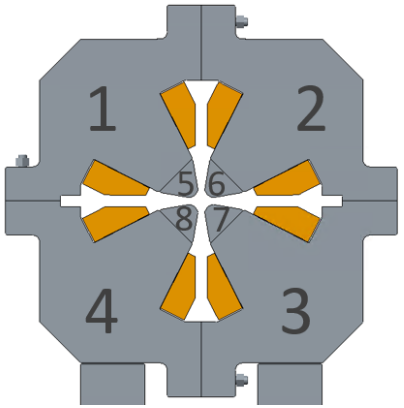

Magnet Yoke

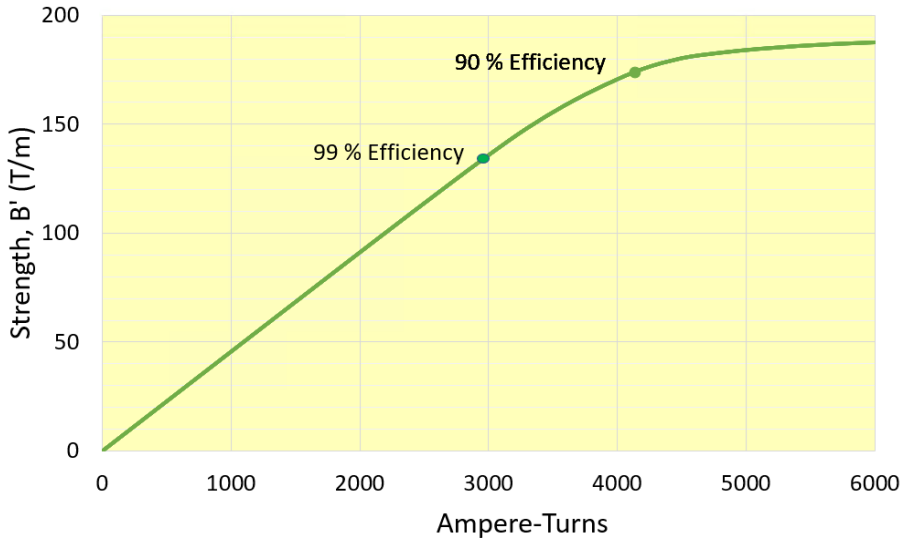

NSLS-IIU Quadrupole

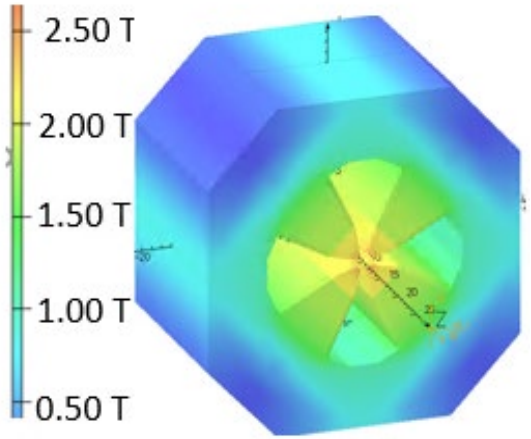

Flux Plot

High Strength Sextupoles

Facility	APSU	ALSU	DLS-II	ESRF-EBS	HEPS	Soleil-U	PETRA-IV
B''/2 (T/m^2)	3038	2607	5000	1716	3340	8100	2250
Bore R (mm)	14	12	12	19.2	13	8	11

- Small bore radius
- Solid yoke of soft iron except Soleil-U (laminated steel)
- High permeability FeCo (Vanadium Permendur, Vacoflux) pole tips where necessary
- H, V correction coils are normally included
- Field uniformity ($\Delta S/S_0 < 10^{-2}$ to 10^{-3})
- Pole-tip gap > 6 mm for vacuum chamber and x-ray exit

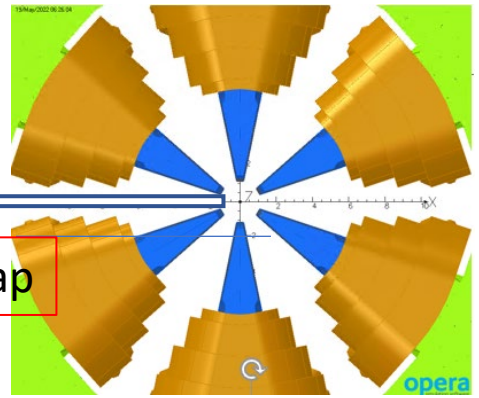

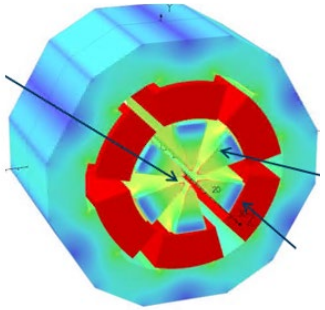

ALSU (SFA)

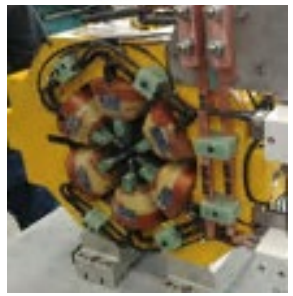

APSU (S2)

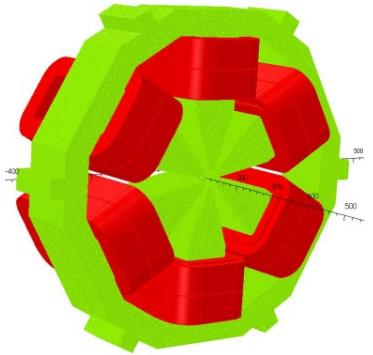

PETRA IV (PSA)

High Strength Sextupole (contd.)

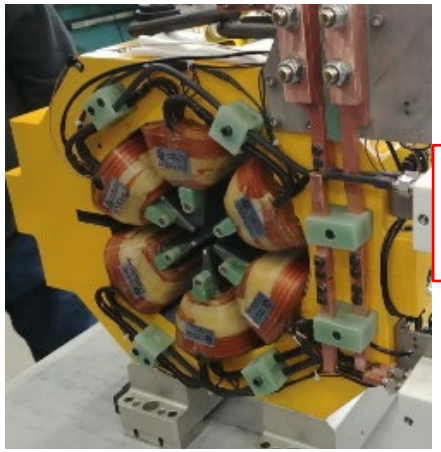

APSU – S2

Bore radius/Pole-tip gap ≥ 1.4 for good field harmonics.

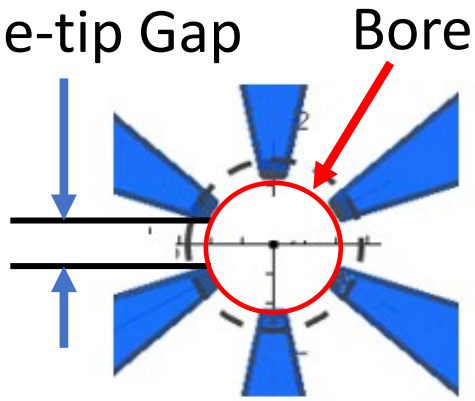

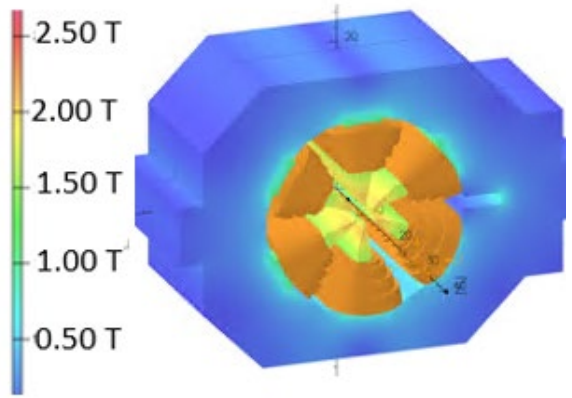

- The pole-tip gap of the APSU S2 sextupole was reduced from 10 mm to 8 mm
- The bore radius was reduced from 14 mm to 11 mm
- The sextupole strength (B’’/2) reaches 6,200 T/m^2 at 98% efficiency level
- At R_{ref} = 3 mm, B_8 (18-pole) = 1.0 e-04, is the only harmonic greater than 0.01 e-04

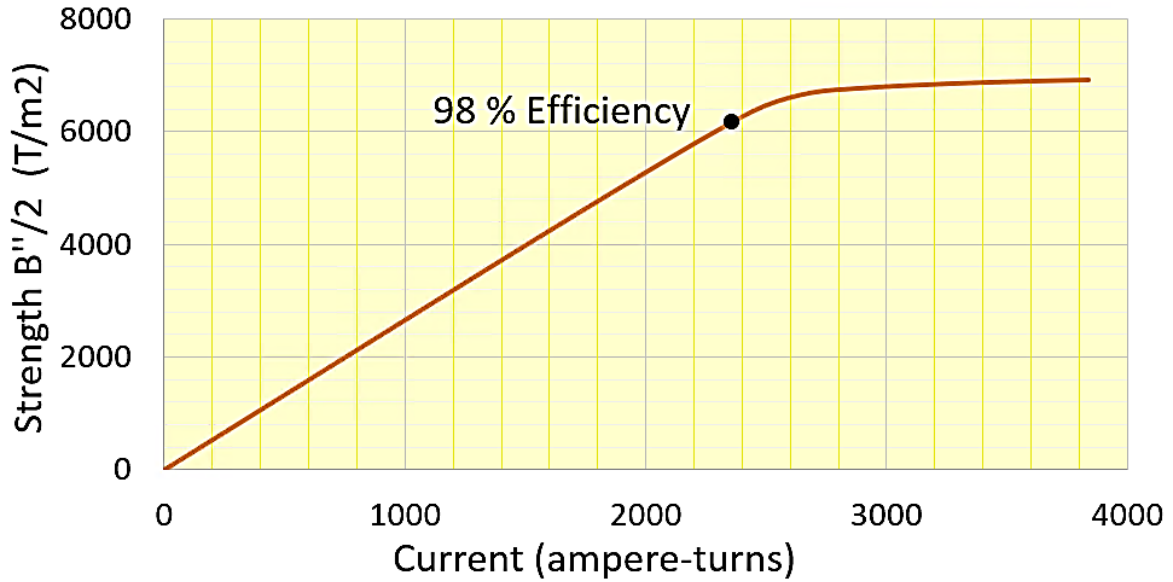

High Strength Octupole/Corrector

Facility	DLS-II	ESRF-EBS	HEPS	PETRA-IV	Soleil-U	SPring-8-II
B’’’/6 (T/m^3)	70 e03	72 e03	85 e03	120 e03	100 e03	24 e03
Bore R (mm)	14	NA	13	11	8	25

- Small bore radius
- Solid yoke of soft iron (1010), except Soleil-U(laminated steel)
- Air-cooled coils
- APSU 8-pole corrector can be converted into an octupole by reconfiguring power supply connections.

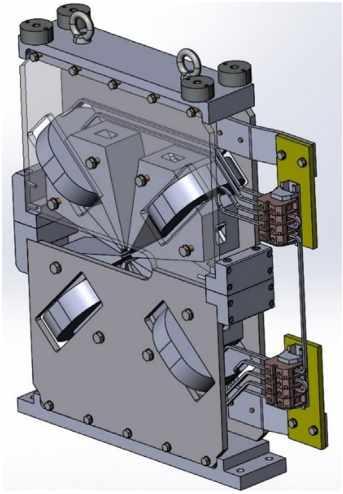

PETRA IV Octupole[1]

Soleil-U Octupole

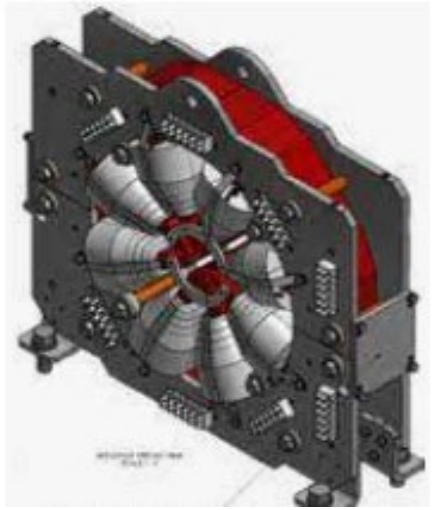

APSU Corrector/Octupole

[1] *A. Aloev, PETRA IV TAC Meeting, March 2022*

APSU Corrector/Octupole

Dipole (H,V) and Skew Quad Corrector

Parameter	Value
Bore radius	15.5 mm
Yoke (laminated) length	84.6mm
DC correction	0.44 mrad
Steering (1 kHz)	4.4 µrad
Integ. skew gradient	0.73 T

NSLS-IIU Octupole:

- Bore radius: 14 mm
- Pole-tip gap: 8 mm
- Solid Yoke: 206 mm x 206 mm
- Octupole strength (B’’’/6) = 121,000 T/m^3
- (Efficiency of 99%)

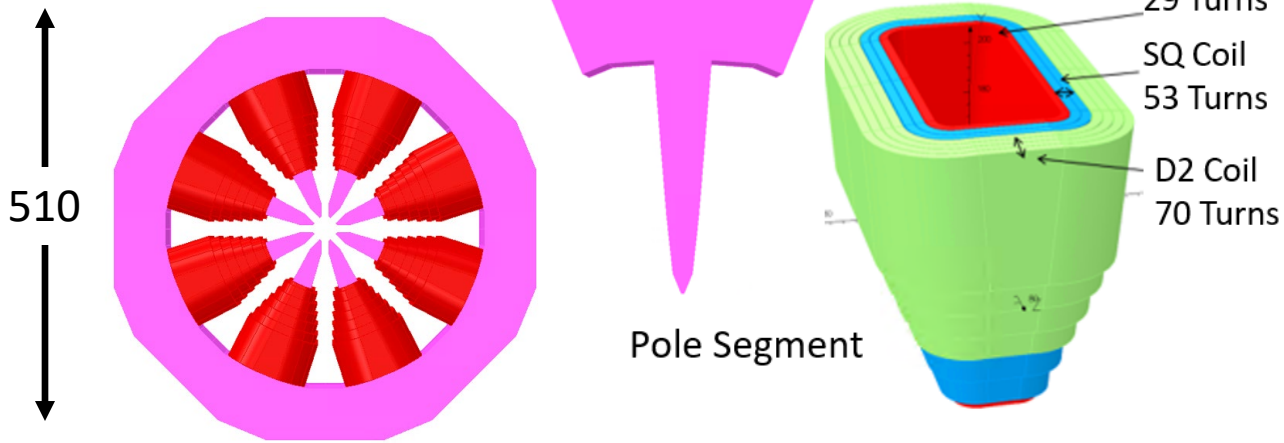

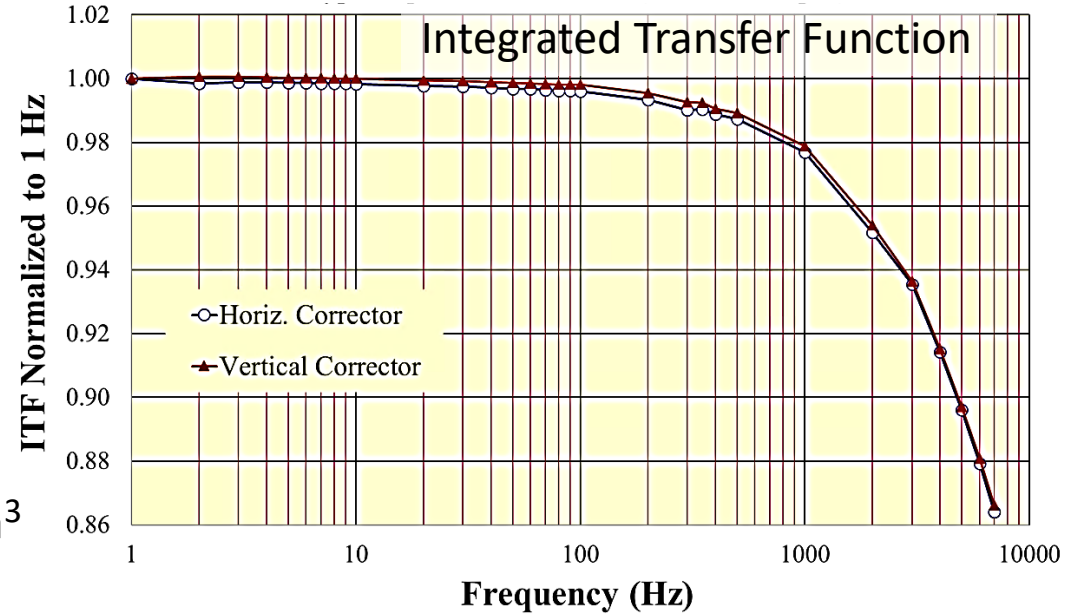

At 1 kHz. drop in ITF = 2%, phase lag < 4^o

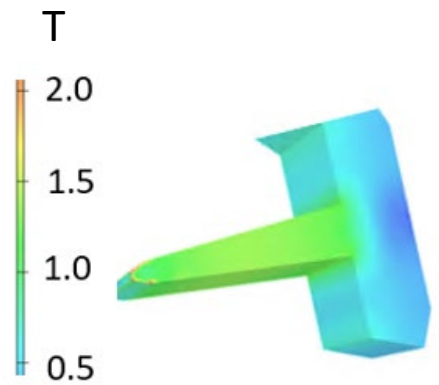

Flux plot
NSLS-IIU Octupole

Concluding Remarks

- 4GSR are based on moderate strength dipoles and high strength multipoles.
- Hybrid PM dipoles, successfully implemented at ESRF-EBS, are now common in the upgrade plans of most of the facilities.
- There are technical challenges in extending the PM technology to high strength quadrupoles. R&D is underway at NSLS-II on high-field PMQs, field harmonics correction, magnet alignment, magnetic measurements, vacuum chamber and x-ray beam extraction, and long-term radiation damage of PM materials.
- Preliminary designs of Halbach-style and hybrid-PM of high field strength (130 T/m) for the NSLS-IIU complex bend lattice were presented.
- The higher field strength requirements of the EM multipoles of future 4GSR can be met by reducing the bore radii of the APSU-style magnets.

Thank you for your attention